

Spin-current manipulation of photoinduced magnetization dynamics in heavy metal / ferromagnet double layer based nanostructures

Steffen Wittrock¹, Dennis Meyer², Markus Müller², Henning Ulrichs², Jakob Walowski³, Maria Mansurova³, Ulrike Martens³, and Markus Münzenberg³

¹Unité Mixte de Physique CNRS/Thales, Université Paris Sud, 1 Avenue Augustin Fresnel, 91767 Palaiseau, France

²I. Physikalisches Institut, Georg-August-Universität Göttingen, Friedrich-Hund-Platz 1, 37077 Göttingen, Germany

³Institut für Physik, Ernst-Moritz-Arndt-Universität Greifswald, Felix-Hausdorff-Str. 6, 17489 Greifswald, Germany

Spin currents offer a way to control static and dynamic magnetic properties, and therefore they are crucial for next-generation MRAM devices or spin-torque oscillators. Manipulating the dynamics is especially interesting within the context of photo-magnonics. In typical 3d transition metal ferromagnets like CoFeB, the lifetime of light-induced magnetization dynamics is restricted to about 1 ns, which e.g. strongly limits the opportunities to exploit the wave nature in a magnonic crystal filtering device. Here, we investigate the potential of spin-currents to increase the spin wave lifetime in a functional bilayer system, consisting of a heavy metal (8 nm of β -Tantalum (Platinum)) and 5 nm CoFeB. Due to the spin Hall effect, the heavy metal layer generates a transverse spin current when a lateral charge current passes through the strip. Using time-resolved all-optical pump-probe spectroscopy, we investigate how this spin current affects the magnetization dynamics in the adjacent CoFeB layer. We observed a linear spin current manipulation of the effective Gilbert damping parameter for the Kittel mode from which we were able to determine the system's spin Hall angles. Furthermore, we measured a strong influence of the spin current on a high-frequency mode. We interpret this mode as an exchange dominated higher order spin-wave resonance. Thus we infer a strong dependence of the exchange constant on the spin current.

Index Terms—Spin Hall effect, spin current, magnetization dynamics, magneto-optical Kerr-effect.

I. INTRODUCTION

THE spin-transfer effect describes the transfer of spin angular momentum to a ferromagnet's magnetization from an injected spin polarized current. Since its prediction by L. Berger [1], this effect has experienced a high research interest as it permits to manipulate and control the magnetization of a thin ferromagnetic (FM) layer. Especially when the resulting spin transfer torque is collinear with the damping torque, magnetic dissipation can be controlled. Thereby the life time of spin wave dynamics can be drastically enhanced.

Among the possible methods of creating the necessary spin current, the exploitation of the spin Hall effect has become a powerful mean since its first observation only a decade ago [2], [3], [4], [5]. Governed by spin-orbit coupling phenomena, it generates a spin current j_s from a transverse charge current j_e without any need for neither a ferromagnet nor an external magnetic field. The efficiency of the conversion process can be described by the spin Hall angle (SHA) $\Theta_{SH} = j_s/j_e$.

Here, we investigate the photo-induced magnetization dynamics in a few nanometer thin soft magnetic layer consisting of amorphous metallic cobalt iron boron alloy ($\text{Co}_{20}\text{Fe}_{60}\text{B}_{20}$) under influence of a strong spin current generated by the SHE in an adjacent heavy metal film made of platinum (Pt) or tantalum (Ta). The sputter conditions for Ta were chosen such that the film has grown in the high resistive β -phase for which a high SHA has recently been reported [6].

II. EXPERIMENTAL

The samples consist of two functional thin layers (fig. 1a): 8 nm Pt or β -Ta as a SHE-material generating the spin current

and 5 nm of ferromagnetic amorphous CoFeB, into which the spin current is being injected in order to manipulate its magnetization dynamics. The layer stack is complemented by 3 nm of Ru as a capping layer. CoFeB and Ta are deposited by argon ion sputtering and Pt and Ru by e-beam evaporation. All preparation steps are conducted in situ in ultra-high vacuum. Subsequent structuring of the samples by e-beam lithography enables the electrical contacting and generation of a high charge current density (fig. 1b).

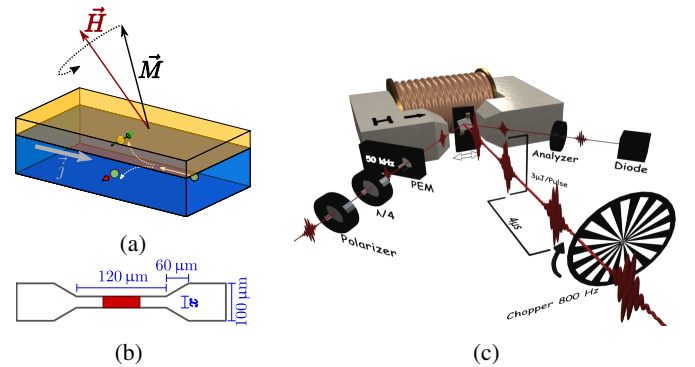


Fig. 1: Experimental characteristics. (a) Schematic processes in the functional layer stack of a SHE material (blue) and the ferromagnetic CoFeB (yellow). (b) Patterned sample structure, the width x was 12 μm for the results shown here. The red marked area was excited by the laser spot. (c) Pump-probe setup with ratio of powers $P_{\text{pump}} : P_{\text{probe}} = 95 : 5$, time resolution is realized by a delay stage, a double modulation technique of photoelastic modulator (PEM) and chopper frequency was used [7].

the magneto-optical Kerr effect to excite and measure magnetization dynamics (schematic setup in 1c). The laser pulses with central wave length $\lambda = 800$ nm have an autocorrelation length of $\Delta\tau \approx 80$ fs and a repetition rate of 250 kHz. The pump spot size was ≈ 60 μm providing an optical fluence of $F = 15 \text{ mJ}/\text{cm}^2$.

The incoming pump pulse induces the dynamics at $\tau = 0$ by firstly generating hot electrons, which thermalize on a timescale of $\tau \sim 100$ fs due to electron-electron-scattering. Further scattering events with phonons and spins lead to energy transfer into the phonon and spin system giving rise to ultrafast demagnetization [8]. Caused by the high change in temperature on the time scale of ~ 1 ps, the local anisotropy constant of the ferromagnetic material and thus the effective magnetic field \vec{H}_{eff} is changed. With \vec{H}_{eff} rereaching its equilibrium position after a few picoseconds, the magnetization dynamics corresponding to the Landau-Lifshitz-Gilbert-equation (LLG) is excited. In order to subsequently trigger a coherent precession of the magnetization, an external field (145 mT) was applied at an out-of-plane angle of $\varphi = 35^\circ$, transversal to \vec{j}_e .

III. RESULTS - NANOSECOND TIMESCALE

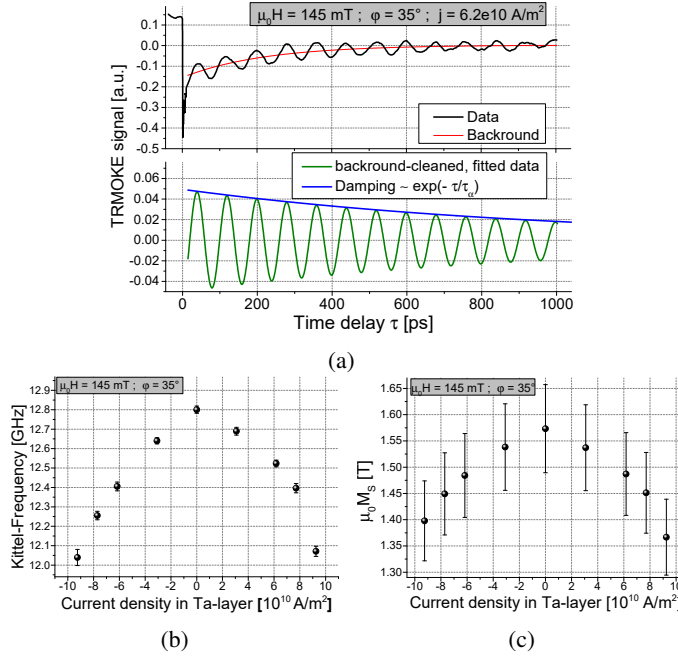


Fig. 2: (a) Typical measurement data and Kittel mode after subtraction of exponential background. The TRMOKE-signal is proportional to the magnetization. Dependence of (b) Kittel frequency and (c) saturation magnetization on the current density in the Ta-layer.

Besides the dominating coherent, in spatially homogeneous geometries called Kittel mode oscillations, also incoherent phonons and magnons contribute to the signal and give rise to a certain background [9], [8], which can be modelled by exponential functions. Subtracting it from the raw data (fig. 2) highlights the magnetic oscillations. These are analysed

with respect to frequency and damping for different current densities passing through the SHE-material.

A. Kittel frequencies, magnetization, and Oersted field

The dependence of the Kittel frequency on j is shown in fig. 2b. The mainly parabolic behaviour can be attributed to the reduction of the saturation magnetization due to Joule-heating. The observable asymmetries for opposite current directions can be related to the Oersted field produced by the current, or to the presence of a field-like torque. Analysing the asymmetries, an Oersted field of $H_{Oe} = aj$ with $a = (1.23 \pm 0.04) \cdot 10^{-8} \text{ m}$ is determined which agrees well with theoretical estimations. Even if present, the field-like torque must be much smaller than the effect arising from the Oersted field. Taking also into account the in-plane applied magnetic field component H_x , the saturation magnetization can be determined from the Kittel formula $\omega = \gamma\mu_0\sqrt{H_x(H_x + M_S)}$ (fig. 2c). Note that for the given field geometry, the magnetization's out-of-plane component is only around 2%, as is estimated by micromagnetic simulations; therefore this approximation is valid. Besides Joule-heating, also the energy deposition of the pump pulse heats up the sample locally to around 400-450 K at a time scale of up to 1 ns. Thus the saturation magnetization at $j = 0 \text{ A/m}^2$ is slightly lower than the room temperature value of $\mu_0 M_S = 1.63 \text{ T}$, determined by a vibrating sample magnetometer [10]. The Joule-heating effect leads to a temperature increase especially in Ta of up to 200 K at a maximum current density of $j_{Ta} = 9.3 \cdot 10^{10} \text{ A/m}^2$.

B. Effective Gilbert damping parameter of the Kittel mode

From the exponential decay time τ_α of the Kittel mode (fig. 2a) and taking into account the full in-plane magnetic field $H_x = H_{ext} \cos(\varphi) + H_{Oe}$, and the current dependence of the magnetization, we calculate the effective Gilbert damping parameter using:

$$\alpha_{Kittel} = \left(\tau_\alpha \gamma \mu_0 \left(H_x + \frac{M_S}{2} \right) \right)^{-1}. \quad (1)$$

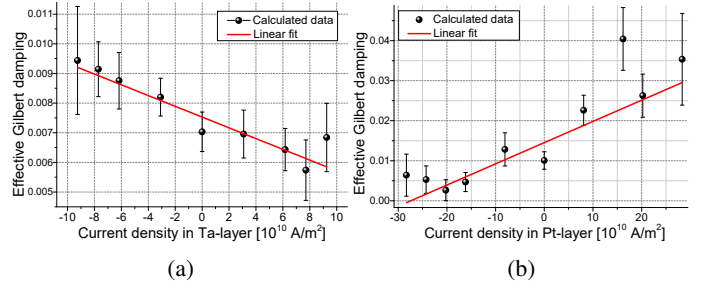


Fig. 3: Current dependence of the effective Gilbert damping parameter for (a) the Ta based sample and (b) the Pt based sample. From the linear fit, the SHE efficiency can be extracted.

Results for the two SHE-materials Ta and Pt are shown in fig. 3. We determined the SHA Θ_{SH} by fitting the formula:

$$\tilde{\alpha} = \alpha + j \cdot \Theta_{SH} \cdot \frac{\hbar}{2ed\mu_0 M_S H_x}. \quad (2)$$

Note that this expression was derived from linearizing the Landau-Lifshitz-Gilbert-Slonczewski-equation (LLGS).

Averaging a few datasets gives the SHAs of:

$$\Theta_{SH}^{Ta} = -0.043 \pm 0.011 \quad ,$$

and

$$\Theta_{SH}^{Pt} = 0.086 \pm 0.012 \quad .$$

These results lie within the values obtained by other groups [11] and in particular confirm the different sign to be expected for Pt [12], [13] and Ta [14], [6].

C. Spin-pumping effect

The spin mixing conductance $g^{\uparrow\downarrow}$ of a layer combination can be estimated through comparison of the effective damping parameters $\tilde{\alpha}$ of two layer stacks involving the same ferromagnetic material. Using Ta and Pt as SHE-materials and CoFeB as the ferromagnet, the spin mixing conductance of Ta can be calculated using:

$$g_{Ta}^{\uparrow\downarrow} = -\frac{4\pi M_S d \cdot \Delta\tilde{\alpha}}{\hbar\gamma} + g_{Pt}^{\uparrow\downarrow} \quad (3)$$

$\Delta\tilde{\alpha} = \tilde{\alpha}_{Pt} - \tilde{\alpha}_{Ta}$ denotes the difference of the effective magnetic damping constants of the $d = 5$ nm thick CoFeB layer for the two different adjacent SHE-materials. Average values of a few measurements give $\tilde{\alpha}_{Pt} = (1.20 \pm 0.15) \cdot 10^{-2}$ and $\tilde{\alpha}_{Ta} = (0.69 \pm 0.05) \cdot 10^{-2}$ for $j = 0$. The Pt/CoFeB spin mixing conductance of $g_{Pt}^{\uparrow\downarrow} = (4 \pm 1) \cdot 10^{19} \text{ m}^{-2}$ [18] was used as a reference value.

We evaluate the spin mixing conductance of Ta/CoFeB to $g_{Ta}^{\uparrow\downarrow} = (1.9 \pm 1.2) \cdot 10^{19} \text{ m}^{-2}$. The smaller value for Ta/CoFeB compared to Pt/CoFeB is expected as similar values were already obtained in Ta/NiFe [15] resp. Pt/NiFe [16] bilayers. In conclusion, this analysis shows that TRMOKE is also a suitable method to determine the spin mixing conductance which is an important parameter for heavy metal/FM based bilayer systems.

IV. RESULTS - PICOSECOND TIMESCALE

On the timescale of a few picoseconds, when the magnetization starts relaxing again, we observed a strongly damped, ultrafast oscillation in the terahertz regime (fig. 4c), usually existent for one or two periods (fig. 4). We identified this oscillation as the well-known perpendicular standing spin-wave (PSSW) mode of first order $n = 1$. Analysing its frequencies (fig. 4c) and taking into account the saturation magnetization gathered on the nanosecond timescale, especially the exchange stiffness A (fig. 4d) can be obtained from:

$$\omega = \gamma\mu_0 \sqrt{\left(H_x + \frac{2A}{\mu_0 M_S} k^2\right) \left(H_x + \frac{2A}{\mu_0 M_S} k^2 + M_S\right)} \quad (4)$$

with $k^2 = k_z^2 = (n\pi/d)^2$, $n \in \mathbb{N}$ the quantized wavevector normal to the plane. The exchange stiffness is shown in fig. 4d and found to depend on the spin current.

Note that pinning at interfaces can alter the effective wave length of the exchange mode. Without further experimental evidence, assuming zero pinning is the simplest model. Since the exchange constant fits to known values determined from TRMOKE experiments on thicker films [17], we stick to this model.

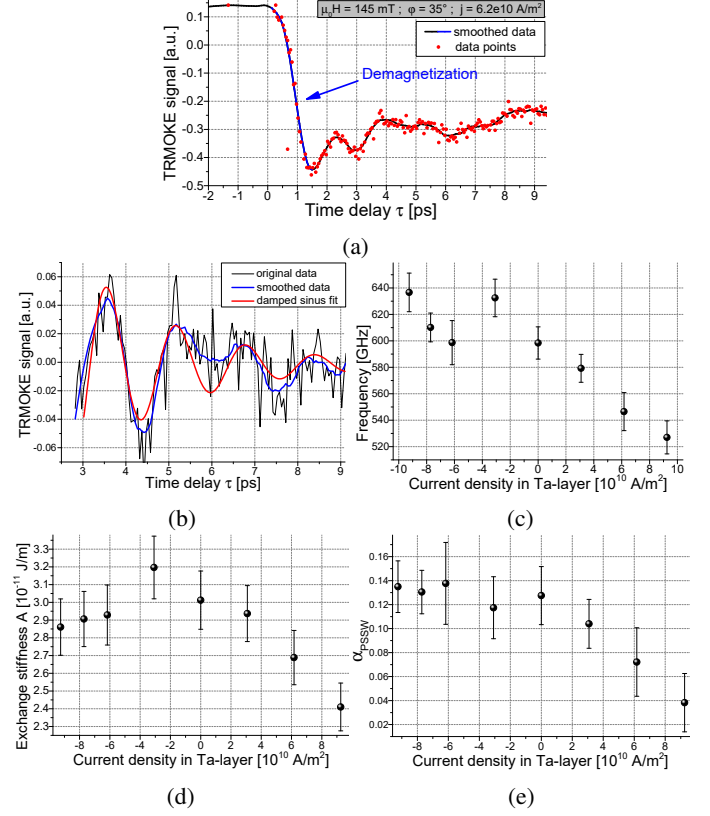


Fig. 4: (a) The first ten picoseconds of the excited dynamics including an ultrafast, highly damped oscillation during re-magnetization (b). (c-e) Current dependence of certain derived parameters.

The Gilbert damping parameter of the PSSW mode (fig. 4e) can again be determined from the oscillation's exponential decay time τ_α :

$$\alpha_{PSSW} = \left(\tau_\alpha \gamma \mu_0 \left(H_x + \frac{2Ak^2}{\mu_0 M_S} + \frac{M_S}{2} \right) \right)^{-1} \quad (5)$$

Especially the exchange term $\sim Ak^2/M_S$ proves to be dominant due to the small CoFeB thickness. We attribute the (at least for positive j_{Ta}) linear behaviour of α_{PSSW} to the SHE. The curve's slope (fig. 4e, $j_{Ta} \geq 0$) possesses the same sign as the Kittel mode damping α_{Kittel} . Furthermore, α_{PSSW} is found to be one order of magnitude higher than α_{Kittel} . The relative change from $\alpha_{PSSW} \approx 0.04$ for a high positive current density up to $\alpha_{PSSW} \approx 0.13$ for $j = 0$ shows a strong dependence on the spin current which is around three times higher than for the Kittel mode.

V. DISCUSSION

According to our experiments, the SHA for a Pt-based layer structure is almost double the SHA of the Ta-system. A strong

Joule-heating effect occurred especially in the Ta based structure because of its high resistivity. The latter also contributes to an eventual systematic reduction of the tantalum's SHA by up to 10 % assuming the capped Ru displays a small negative SHA of $\Theta_{SH} \approx -0.001$ [19]. This would lead to a spin current with opposing sign flowing into the CoFeB from above.

The strong spin pumping mechanism and thus increase of the magnetic damping constant especially in the Pt sample is theoretically expected due to platinum's high spin flip probability. Adding an interlayer with high spin diffusion length (such as Cu [20], [21], [22]) could solve this issue.

The interesting discovery of the fast, highly damped magnetic oscillation within the first 10 ps of the remagnetization process is identified as the PSSW mode of first order. It shows a strong dependence on the injected spin current which influences its frequency, the exchange stiffness and the mode's damping. Note that usually, the PSSW mode is optically excitable and observable in samples, whose layer thickness is higher than the optical penetration depth which is ~ 30 nm in our case. To obtain clear evidence of this mode's properties, further investigations with enhanced signal to noise ratio are necessary.

VI. CONCLUSION AND OUTLOOK

In this article we discussed the photoinduced magnetization dynamics under influence of an injected spin current, generated by the SHE. The powerful tool of time resolved magneto-optical Kerr effect, compared to more established methods like BLS or ST-FMR, allowed to investigate nanosecond as well as (sub-)picosecond dynamics and to get insights into high-frequency and non-equilibrium dynamics so far not in the focus within this context.

We discussed the influence of Joule-heating on our samples and described the linear manipulation of the Kittel mode's Gilbert damping through a spin current. The spin Hall angles which could be determined for the two different, commonly used SHE materials Ta and Pt, lie within other reported values [11].

We reported a magnetic oscillation at the picosecond timescale which is found to be highly dependent on the spin current. The exact behaviour of this mode has to be further investigated in future experiments with enhanced signal to noise ratio. Furthermore, the interesting timescales of the demagnetization process will be addressed in future publications.

Standard methods such as ST-FMR do not allow to address such high-frequency dynamics easily. Our approach enables us to enter this temporal regime, which provides new insights on the action of spin torques on picosecond time scales.

ACKNOWLEDGMENT

The authors acknowledge financial support by the DFG, within the CRC 1073 'Atomic scale control of energy conversion'.

REFERENCES

- [1] BERGER, L.: *Exchange interaction between ferromagnetic domain wall and electric current in very thin metallic films*. Journal of Applied Physics 55, 6, p. 1954-1956, 1984.
- [2] KATO, Y.K.; MYERS, R.C.; GOSSARD, A.C.; AWSCHALOM, D.D.: *Observation of the Spin Hall Effect in Semiconductors*. Science 306, 5703, p. 1910-1913, 2004.
- [3] WUNDERLICH, J.; KÄSTNER, B.; SINOVA, J.; JUNGWIRTH, T.: *Experimental discovery of the spin-Hall effect in Rashba spin-orbit coupled semiconductor systems*. condmat/0410295.
- [4] DAY, C.: *Two Groups Observe the Spin Hall Effect in Semiconductors*. Phys. Today 58, 2, 17, 2005.
- [5] WUNDERLICH, J.; KÄSTNER, B.; SINOVA, J.; JUNGWIRTH, T.: *Experimental observation of the spin-Hall effect in a two-dimensional spin-orbit coupled semiconductor system*. Physical Review Letters, 94(4), 047204, 2005.
- [6] LIU, L.; PAI, C.-F.; LI, Y.; TSENG, H. W.; RALPH, D. C.; BUHRMAN, R. A.: *Spin-torque switching with the giant spin Hall effect of tantalum*. Science 336, 6081, 2012.
- [7] KOOPMANS, B.: *Laser-Induced Magnetization Dynamics*. In: HILLEBRANDS, B.; OUNADJELA, K.: *Spin Dynamics in Confined Magnetic Structures II*, 2003.
- [8] BEAUREPAIRE, E.; MERLE, J.-C.; DAUNOIS, A.; BIGOT, J.-Y.: *Ultrafast Spin Dynamics in Ferromagnetic Nickel*. Phys. Rev. Lett. 76, p. 4250-4253, 1996.
- [9] DJORDJEVIC, M.; LÜTTICH, M.; MOSCHKAU, P.; GUDERIAN, P.; KAMPFRATH, T.; ULBRICH, R. G.; MÜNZENBERG, M.; FELSCH, W.; MOODERA, J. S.: *Comprehensive view on ultrafast dynamics of ferromagnetic films*. Physica status solidi (c) 3, 5, p. 1347-1358, 2006.
- [10] MANSUROVA, M.: *Magnetization and elastic dynamics in nanostructured metamaterials*. I. Physikalisches Institut, Georg-August-Universität Göttingen, 2016.
- [11] SINOVA, J.; VALENZUELA, S.O.; WUNDERLICH, J.; BACK, C.H.; JUNGWIRTH, T.: *Spin Hall effects*. Reviews of Modern Physics 87, 4, p. 1213-1260, 2015.
- [12] LIU, L.; MORIYAMA, T.; RALPH, D.C.; BUHRMAN, R.A.: *Spin-Torque Ferromagnetic Resonance Induced by the Spin Hall Effect*. Phys. Rev. Lett. 106, 036601, 2011.
- [13] ANDO, K.; TAKAHASHI, S.; HARI, K.; SASAGE, K.; IEDA, J.; MAEKAWA, S.; SAITO, E.: *Electric Manipulation of Spin Relaxation Using the Spin Hall Effect*. Phys. Rev. Lett. 101, 036601, 2008.
- [14] MOROTA, M.; NIIMI, Y.; OHNISHI, K.; WEI, D.H.; TANAKA, T.; KONTANI, H.; KIMURA, T.; OTANI, Y.: *Indication of intrinsic spin Hall effect in 4d and 5d transition metals*. Phys. Rev. B 83, 174405, 2011.
- [15] MONTROYA, E.; OMELCHENKO, P.; COUTTS, C.; LEE-HONE, N.R.; HÜBNER, R.; BROUN, D.; HEINRICH, B.; GIRT, E.: *Spin transport in tantalum studied using magnetic single and double layers*. Phys. Rev. B 94, 054416, 2016.
- [16] CZESCHKA, F.D.; DREHER, L.; BRANDT, M.S.; WEILER, M.; ALTHAMMER, M.; IMORT, I.-M.; REISS, G.; THOMAS, A.; SCHOCH, W.; LIMMER, W.; HUEBL, H.; GROSS, R.; GOENNENWEIN, S.T.B.: *Scaling behavior of the spin pumping effect in ferromagnet/platinum bilayers*. arXiv:1012.3017, 2011.
- [17] ULRICH, S.; LENK, B.; MÜNZENBERG, M.: *Magnonic spin-wave modes in CoFeB antidot lattices*. Appl. Phys. Lett. 97, 092506, 2010.
- [18] RUIZ-CALAFORRA, A.; BRÄCHER, T.; LAUER, V.; PIRRO, P.; HEINZ, B.; GEILEN, M.; CHUMAK, A.V.; CONCA, A.; LEVEN, B.; HILLEBRANDS, B.: *The role of the non-magnetic material in spin pumping and magnetization dynamics in NiFe and CoFeB multilayer systems*. Journal of Applied Physics 117, 16, 2015.
- [19] KAMPFRATH, T.; BATTIATO, M.; MALDONADO, P.; EILERS, G.; NÖTZOLD, J.; MÄHRLEIN, S.; ZBARSKY, V.; FREIMUTH, F.; MOKROUSOV, Y.; BLÜGEL, S.; WOLF, M.; RADU, I.; OPPENEER, P.M.; MÜNZENBERG, M.: *Terahertz spin current pulses controlled by magnetic heterostructures*. Nature nanotechnology 8, 4, p. 256260, 2013.
- [20] MIZUKAMI, S.; ANDO, Y.; MIYAZAKI, T.: *Effect of spin diffusion on Gilbert damping for a very thin permalloy layer in Cu/permalloy/Cu/Pt films*. Phys. Rev. B 66, 104413, 2002.
- [21] SUN, Y.; CHANG, H.; KABATEK, M.; SONG, Y.-Y.; WANG, Z.; JANTZ, M.; SCHNEIDER, W.; WU, M.; MONTROYA, E.; KARDASZ, B.; HEINRICH, B.; VELTHUIS, S.G.E.; SCHULTHEISS, H.; HOFFMANN, A.: *Damping in Yttrium Iron Garnet Nanoscale Films Capped by Platinum*. Phys. Rev. Lett. 111, 106601, 2013.
- [22] ROJAS-SÁNCHEZ, J.-C.; REYREN, N.; LACZKOWSKI, P.; SAVERO, W.; ATTANÉ, J.-P.; DERANLOT, C.; JAMET, M.; GEORGE, J.-M.; VILA, L.; JAFFRÈS, H.: *Spin Pumping and Inverse Spin Hall Effect in Platinum: The Essential Role of Spin-Memory Loss at Metallic Interfaces*. Phys. Rev. Lett. 112, 106602, 2014.